Materials Corrosion and Mitigation Strategies for APT, Weapons Neutron Research Facility Experiments:

The Effects of 800 MeV Proton Irradiation on the Corrosion of Tungsten, Tantalum, Stainless Steel, and Gold

R. Scott Lillard, Darryl P. Butt
Materials Corrosion & Environmental Effects Laboratory
MST-6, Metallurgy

Gary Kanner
MST-6, Metallurgy

Luke Daemen
LANSCE-LER

Los Alamos National Laboratory
Los Alamos, New Mexico 87545

submitted to:

Laurie Waters
APT Project Office

December 1, 1997

contributors:
Donald Pile, MST-6
Gordon Willcutt, TSA-10
Phil Ferguson, LANSCE-LER
John Ullmann, LANSCE-3

Executive Summary

Summary of Results Real time electrochemical data were acquired for tungsten, tantalum, stainless steel 304L, and gold targets during proton irradiation at the LANSCE Weapons Neutron Research Facility. The goal of this research was to establish a better understanding of the corrosion properties of materials as a function of proton irradiation and gain insight into the mechanism of the observed phenomena.

The following electrochemical observations were made during proton irradiation of W, Ta, SS304, and Au:

1) The open circuit potential of all materials increased with increasing proton fluence
2) The corrosion rate (at the OCP) of W and SS304 increased with increasing proton fluence
3) The passive dissolution rate for SS304 and Ta decreased with increasing proton fluence
4) The anodic dissolution rate for W increased with increasing proton fluence
5) The pitting potential for SS304 increased with proton fluence, which is an indication that the material is less susceptible to pitting attack during irradiation.

While no "global" theory of proton beam effects on the electrochemical properties of materials has been established, additional measurements were conducted during the WNR experiments to examine possible mechanisms. To measure the effects of proton irradiation on the passive oxide, Surface Enhanced Raman Spectroscopy (SERS) experiments were conducted on W as a function of proton beam current. SERS, is a powerful technique for examining the properties of the thin (less than 10 $x10^{-9}$ meters thick) oxide which forms on metals. This includes changes in structure, composition, hydration, and oxidation state. Additional experiments which address water radiolysis were also performed. The results of each of these studies (SERS / radiolysis) are reported in separate but attached documents.

To rule out the effects of energy deposition (from the proton beam) on the surface temperature as a possible mechanism for the observed electrochemical effects during irradiation, energy deposition and thermal hydraulic calculations for the rod-shaped tungsten target were performed. The maximum surface temperatures (for a beam current of 484 nA) are 4.8° and 5.1° C above the water temperature (30.8° and 31.1°C). This is only a 0.2% change in surface temperature and, as corrosion rate is proportional to temperature in degrees Kelvin, can not account for the observed electrochemical changes.

The following sections in this Executive Summary provide a brief overview of the results in (1-5) above. The body of the text gives the complete details of all of our WNR corrosion experiments.

Effect of Beam current on the Open Circuit Potential The open circuit potential (OCP) for these materials was measured as a function of time and proton fluence. Typically, when the proton beam was turned on a large positive increase in the OCP was observed. This effect is shown for stainless steel 304 in H_2SO_4 pH 1.6 at a proton beam current of 100 nA in Figure 1.es below. While a positive shift in the OCP is consistent with the formation of radiolysis products such as hydrogen peroxide, the rapid response of the system from beam off to beam on abruptly followed by a plateau in the OCP is not consistent with a steadily increasing concentration of radiolysis products. Moreover, this trend is also consistent with a change in the oxide surface state.

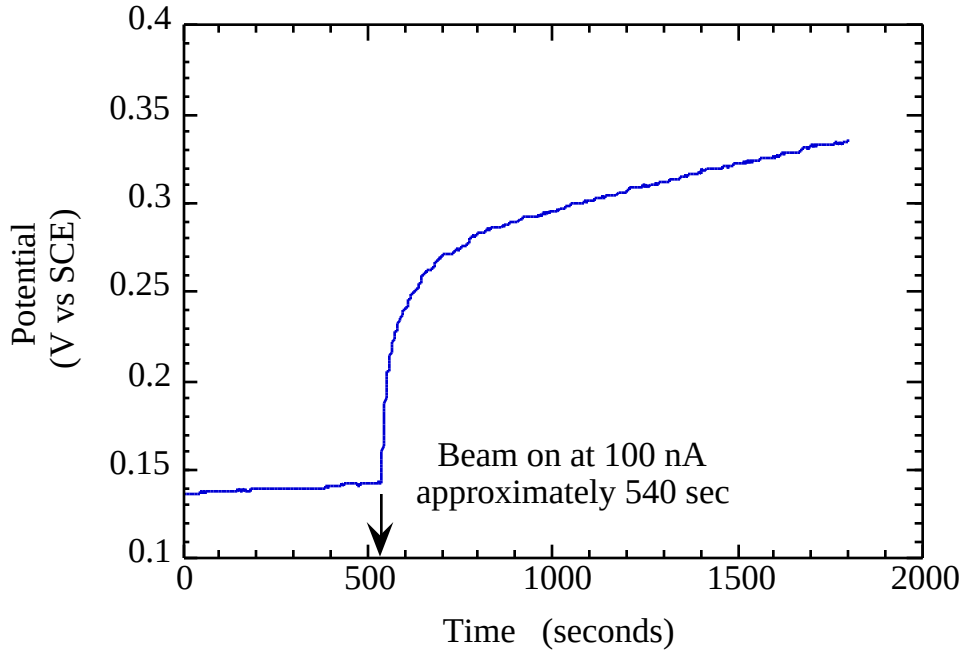

Figure 1.es Open circuit potential for SS304 in flow cell with H_2SO_4. Plot shows pre-beam values and value during irradiation at 100 nA.

Effects of Proton Irradiation on W To distinguish between an increase in cathodic reaction kinetics (which will result from hydrogen peroxide production) and radiation "enhanced" anodic reaction kinetics, EIS experiments for W in 0.10M NaCl (pH 5.2) were performed at an applied anodic potential of 0.0 V SCE. This potential is near the mass transport limited dissolution rate for W. Typical EIS data before the beam was turned on and for beam currents of 141 nA and 484 nA are presented in Figure 2.es in the form of Nyquist plots. Nyquist plots graph the imaginary impedance as a function of the real component of the impedance. As seen in Figure 2.es, there is a precipitous decrease in the low frequency impedance of the tungsten target as beam current is increased. Recall that a decrease in impedance correlates with an increase in metal dissolution rate.

The enhanced dissolution rates observed during in-beam EIS experiments in 0.1M NaCl at applied potentials are complemented by potentiodynamic polarization curves for W generated during irradiation at a proton beam current of 100 nA. In-beam and out-of-beam potentiodynamic polarization curves for W in NaCl (pH 5.2) are presented in Figure 3.es. As shown in this figure both the corrosion rate (dissolution rate at the OCP) and the dissolution rate at applied anodic potentials increase in the presence of proton irradiation.

To summarize, the in-beam W results, both EIS and potentiodynamic polarization experiments found that the anodic dissolution rate of W increased with increasing proton beam current in both pH 1.6 and 5.2 solutions. In addition, potentiodynamic polarization experiments demonstrated that the corrosion rate of W increased with increasing proton beam current in all solutions examined.

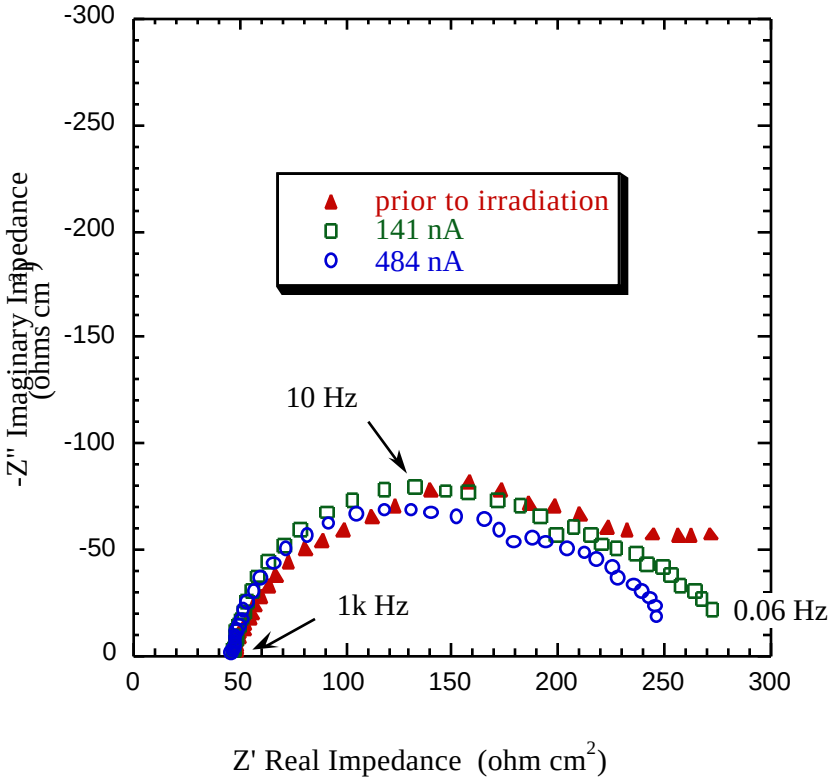

Figure 2.es Nyquist plots for tungsten in 0.10M NaCl as a function of proton beam current.

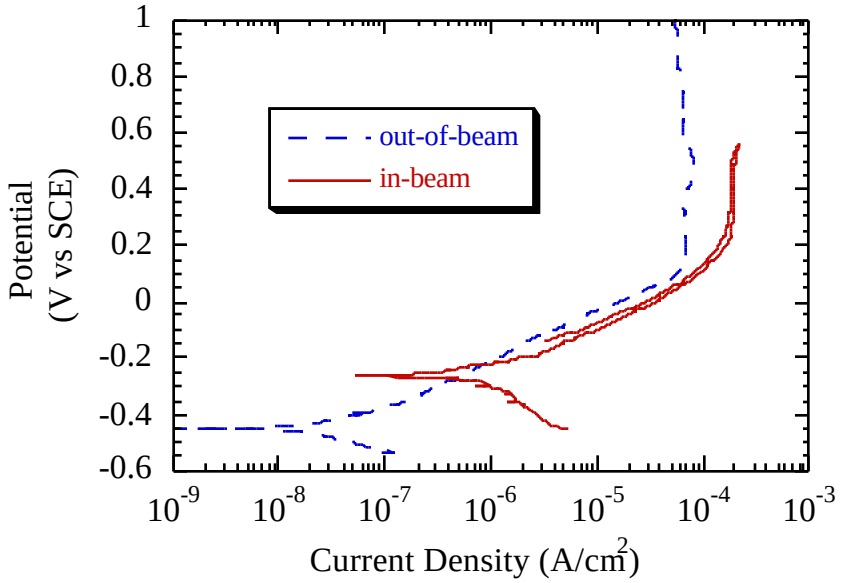

Figure 3.es Potentiodynamic polarization curves for W in 0.1 M NaCl pH 5.2 during irradiation at a proton beam current of 100 nA (in-beam) and with no exposure to irradiation (out-of-beam).

Effects of Proton Irradiation on Stainless Steel 304 In contrast to EIS data for W presented above, the low frequency EIS data for SS304 in sulfuric acid (H_2SO_4) pH 1.6 increases with increasing proton beam current (data not shown). This result was in agreement with potentiodynamic polarization curves for SS304 in this solution (Figure 5.es). In these experiments, the in-beam specimen is associated with a higher OCP at 100nA although the corrosion current density (i_{corr}) appears to be similar to that of the out-of-beam sample. In addition, the passive current density (i_{pass}) for the in-beam appears to be somewhat lower than the out-of-beam sample. Although this difference is small it was reproducible and, in conjunction with the EIS measurements where the charge transfer resistance was found to increase with beam current there is a convincing argument that passive dissolution of SS304 is lowered by interactions with high energy proton irradiation. It is also interesting to note that during the reverse scan a step to lower current densities was observed when the proton beam was shut off. Moreover, this step "returns" the current density to a value identical to that measured for the out-of-beam sample. This is an indication that the electrochemical effects of high energy proton beam interaction with the electrode are reversible.

Additional experiments for SS304 during irradiation were conducted in 0.1M NaCl. Potentiodynamic polarization curves from these experiments are presented in Figure 4.es for samples during irradiation at a proton beam current of 100 nA (in-beam) and not exposed to irradiation (out-of-beam). As can be seen in this figure, while the passive current densities are comparable for the two samples the corrosion current density is somewhat greater for the in-beam sample. In addition, the pitting potential (E_{pit}) for the in-beam sample is 0.662 V while the mean value for 3 out-of-beam samples was 0.495 V +/-37 mV. This is an increase in E_{pit} of approximately 170 mV, a value which is 4.6σ over the mean out-of-beam value indicating that the observed increase is statistically significant. While these results are preliminary, it is an indication that SS304 is less susceptible to pitting attack during irradiation. In comparison, Sikora *et al*

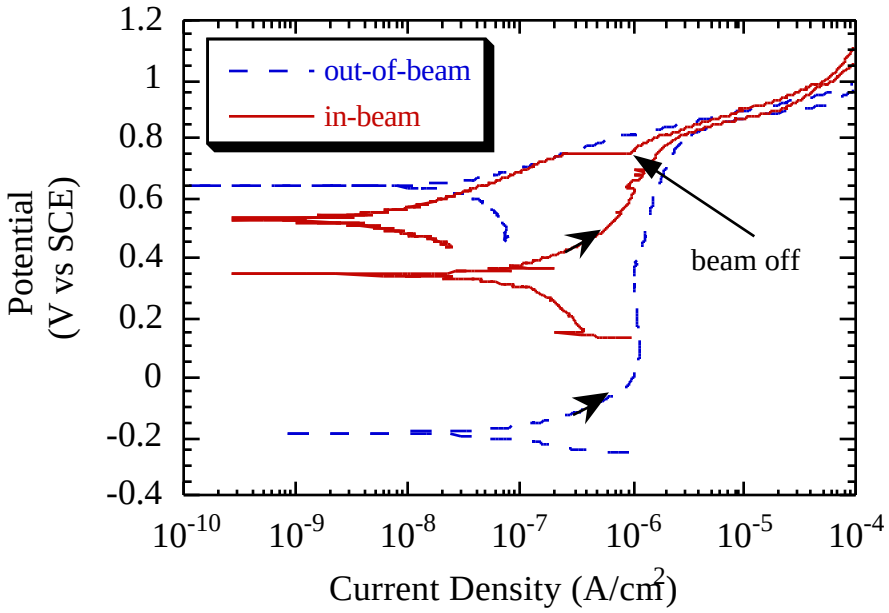

Figure 4.es Potentiodynamic polarization curves for SS304 in H_2SO_4 pH 1.6 for samples during irradiation at a proton beam current of 100 nA (in-beam) and a sample not exposed to irradiation (out-of-beam).

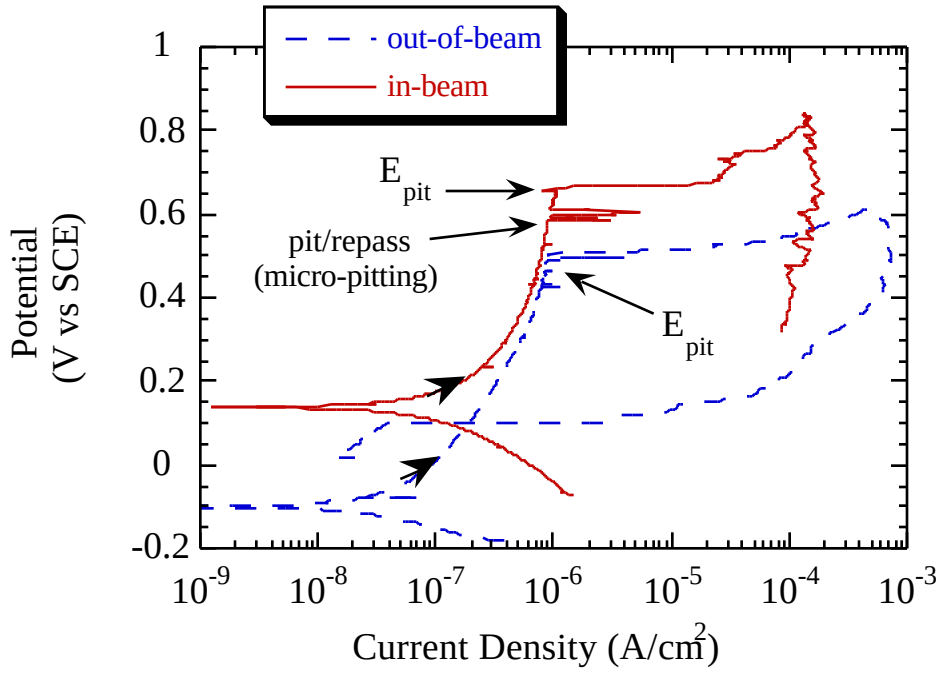

Figure 5.es Potentiodynamic polarization curves for SS304 in 0.1 M NaCl for a sample during irradiation at a proton beam current of 100 nA (in-beam) and a sample not exposed to irradiation (out-of-beam).

found that the pitting potential for SS304 was increased by 60 mV during photon irradiation as compared to samples not exposed to light. It was determined (via Mott Schottky plots) that the increase in pitting potential owed to a change in the conductivity of the passive oxide on SS304. It is also interesting to note that the OCP of the in-beam sample is approximately 50 mV more positive than the repassivation potential (E_{rp}) for the out-of-beam sample. This indicates that once a stable pit is formed, it does not repassivate.

Table of Contents

List of Figures